Title

Efficacy assessment of an active tau immunotherapy in Alzheimers disease patients with amyloid and tau pathology: a post hoc analysis of the ADAMANT randomised, placebo-controlled, double-blind, multi-centre, phase 2 clinical trial.

Permalink

https://escholarship.org/uc/item/77p57133

Authors

Cullen, Nicholas
Novak, Petr
Tosun, Duygu
et al.

Publication Date

2024

DOI

10.1016/j.ebiom.2023.104923

Copyright Information

Peer reviewed

Efficacy assessment of an active tau immunotherapy in Alzheimer's disease patients with amyloid and tau pathology: a post hoc analysis of the "ADAMANT" randomised, placebo-controlled, double-blind, multi-centre, phase 2 clinical trial

Nicholas C. Cullen,[a] Petr Novak,[b,*] Duygu Tosun,[c,d] Branislav Kovacech,[e] Jozef Hanes,[e] Eva Kontsekova,[e] Michal Fresser,[f] Stefan Ropele,[g] Howard H. Feldman,[h] Reinhold Schmidt,[i] Bengt Winblad,[j] and Norbert Zilka[e]

[a]Department of Clinical Sciences, Lund University, Lund, Sweden
[b]Axon Neuroscience CRM Services, Bratislava, Slovakia
[c]San Francisco Veterans Affairs Medical Center, San Francisco, CA, USA
[d]Department of Radiology and Biomedical Imaging, University of California San Francisco, CA, USA
[e]Axon Neuroscience R&D Services, Bratislava, Slovakia
[f]Axon Neuroscience SE, Larnaca, Cyprus
[g]Clinical Division of General Neurology, Department of Neurology, Medical University Graz, Graz, Austria
[h]Department of Neurosciences, Alzheimer's Disease Cooperative Study, University of California San Diego, La Jolla, CA, USA
[i]Clinical Division of Neurogeriatrics, Department of Neurology, Medical University Graz, Graz, Austria
[j]Karolinska Institutet, Department of NVS, Division of Neurogeriatrics, Solna, Sweden and Karolinska University Hospital, Theme Inflammation and Aging, Huddinge, Sweden

Summary

Background Tau pathology correlates with and predicts clinical decline in Alzheimer's disease. Approved tau-targeted therapies are not available.

Methods ADAMANT, a 24-month randomised, placebo-controlled, parallel-group, double-blinded, multicenter, Phase 2 clinical trial (EudraCT2015-000630-30, NCT02579252) enrolled 196 participants with Alzheimer's disease; 119 are included in this post-hoc subgroup analysis. AADvac1, active immunotherapy against pathological tau protein. A machine learning model predicted likely Amyloid+Tau+ participants from baseline MRI. Statistical methods: MMRM for change from baseline in cognition, function, and neurodegeneration; linear regression for associations between antibody response and endpoints.

Results The prediction model achieved PPV of 97.7% for amyloid, 96.2% for tau. 119 participants in the full analysis set (70 treatment and 49 placebo) were classified as A+T+. A trend for CDR-SB 104-week change (estimated marginal means [emm] = −0.99 points, 95% CI [−2.13, 0.13], p = 0.0825]) and ADCS-MCI-ADL (emm = 3.82 points, CI [−0.29, 7.92], p = 0.0679) in favour of the treatment group was seen. Reduction was seen in plasma NF-L (emm = −0.15 log pg/mL, CI [−0.27, −0.03], p = 0.0139). Higher antibody response to AADvac1 was related to slowing of decline on CDR-SB (rho = −0.10, CI [−0.21, 0.01], p = 0.0376) and ADL (rho = 0.15, CI [0.03, 0.27], p = 0.0201), and related to slower brain atrophy (rho = 0.18–0.35, p < 0.05 for temporal volume, whole cortex, and right and left hippocampus).

Conclusions In the subgroup of ML imputed or CSF identified A+T+, AADvac1 slowed AD-related decline in an antibody-dependent manner. Larger anti-tau trials are warranted.

Funding AXON Neuroscience SE.

*Corresponding author. AXON Neuroscience SE, Dvorakovo nabrezie 10, Bratislava 811 02, Slovakia.
E-mail address: petr.novak@axon-neuroscience.eu (P. Novak).

Research in context

Evidence before this study

A range of evidence indicates that tau pathology is closely correlated with and predictive of brain atrophy and clinical decline in Alzheimer's disease and various other tauopathies. Thus, halting or slowing the progression of tau pathology could affect the progression of these disorders, or prevent them if pharmacological intervention occurs at preclinical stages.

Therapies that would halt or slow the progression of tau pathology are not available yet. A wide range of studies report preclinical efficacy of various tau-targeting approaches, though, and numerous tau-targeted drugs are in clinical development.

A search of PubMed using the terms 'tau therapy Alzheimer clinical trial' and 'tau therapy tauopathy clinical trial' conducted on 03-March-2023 did not return any reports clearly demonstrating clinical efficacy of a tau-targeted therapy. Similarly, a search of clinicaltrials.gov and alzforum. org conducted on the same day did not reveal completed phase 3 studies showing efficacy for a tau-targeted drug. This may be due to the fact that tau-targeted drugs are mostly in early development, and have not entered pivotal studies yet. In previous preclinical efficacy studies in rat and mouse models that develop neurofibrillary tau pathology without utilizing mutant tau (tau mutations do not cause Alzheimer's disease), AADvac1 reduced the amount of insoluble tau and tangle pathology in animals, extended their survival, and improved the neurobehavioral phenotype. In the phase 1 studies in humans, the vaccine was shown to be immunogenic and safe. The phase 2 study of AADvac1 in mild AD subjects (MMSE 20–26) showed an impact on neurodegeneration (NfL) and CSF tau markers, but was not sufficiently powered for assessment of clinical efficacy. The population was shown to be negative for tau markers in ~30% of subjects.

This prompted us to conduct a post-hoc analysis of the phase 2 study in subjects most likely to be tau- and amyloid-positive.

Added value of this study

The present post-hoc analysis maximizes the number of evaluable subjects from the ADAMANT dataset by combining available CSF biomarker results and a machine learning approach (whereas the previous manuscript based on this dataset utilized only the sample identified via machine learning). An MMRM model taking into account the entirety of available longitudinal data shows trends towards clinical benefit of AADvac1 treatment in AD. The study demonstrates connections between anti-tau antibody response induced by AADvac1 and longitudinal change in clinical and biomarker assessments of AD—suggesting a dose dependence of effect in the A+T+ subgroup.

Implications of all the available evidence

The present post-hoc analysis is not a conclusive proof of efficacy, and requires validation in a larger cohort of patients positive for tau pathology. The study highlights the need to enrich the populations in trials of tau-targeted drugs using suitable markers of tau pathology, similarly to how trials of anti-amyloid drugs are being enriched using PET and CSF markers of amyloid pathology.

The study supports further investigation of tau-targeted immunotherapies (whether active or passive) for the treatment of Alzheimer's disease.

Developing tau-targeted therapeutics has the potential to deliver efficacious monotherapies, and also enable combining them with therapies aimed at other aspects of AD pathology, such as anti-amyloid, neurotrophic, or immunomodulatory drugs.

Introduction

AADvac1, an active immunotherapy against pathological tau protein, was developed to slow or halt the accumulation of neurofibrillary pathology, and thus to reduce the progression of AD. The vaccine entered clinical development in 2013,[1] with the findings of the phase 2 trial being reported recently.[2] In 2016 when this phase 2 clinical trial was enrolling the 2011 NIA-AA diagnostic framework were state of the art. This framework placed both tau biomarkers and evidence of AD-typical brain atrophy at the same level of importance, under "markers of neuronal injury".[3] As Tau PET was not commercially available at the time of study initiation, and CSF for inclusion not well accepted by patients as well as being logistically challenging at a study-wide level, the ADAMANT trial used evidence of hippocampal atrophy on MRI as an enrichment inclusion criterion for the presence of AD while also accruing a subsample of convenience of those willing to contribute CSF at the time of entry and longitudinally. Subsequent analyses of this CSF subsample identified an overwhelming rate for amyloid positivity (93.3%), but positive results for tau biomarkers only in 70% of cases.[2]

While the primary study objective of ADAMANT demonstrated a favourable safety and tolerability profile with induction of high levels of IgG antibodies, there were no statistically significant effects on cognitive and functional tests on the full sample. In line with this,

study results were equivocal in the entire study sample, but favoured AADvac1 treatment in an amyloid- and tau-positive (A+T+) subgroup. In the current retrospective exploratory study, our aim was to further evaluate this finding by deploying a machine learning imputation model to identify patients as highly likely to be A+T+ based on their MRI volumetry scans, ApoE genotype, demographic and clinical characteristics.[4] Furthermore, we aimed to explore the dose-dependency of these effects by correlating changes in cognition and MRI volumetry with the levels of AADvac1-induced anti-tau IgG antibodies.

Methods

Ethics

All subjects and their caregivers provided written informed consent prior to commencement of study procedures. The study complied with applicable International Council for Harmonisation of Technical Requirements for Pharmaceuticals for Human Use guidelines and the Declaration of Helsinki. The study was approved by the pertinent ethics committees and competent authorities.

The approving ethics committees and approval numbers are as follows: Austria–Ethikkommission der Medizinischen Universität Graz, 28-092 ex 15/16; Czech Republic–Eticka komise Fakultni nemocnice v Motole, EK-1747/15; Germany–Ethik-Kommission II der Universität Heidelberg Universitätsklinikum Mannheim, 2016-001F-MA; Poland–Komisja Bioetyczna przy Bydgoskiej Izbie Lekarskiej, 20/2016; Romania–Comisia Nationala de Bioetica a Medicamentului si a Dispozitivelor Medicale, 159S/21.12.2015; Slovakia–Etická komisia Univerzitnej nemocnice L. Pasteura Košice, EK/15/09; Slovenia–Komisja Republike Slovenije za medicinsko etiko, 0120-307/2016-12; Sweden–Regionala etikprövningsnämnden i Stockholm 2015/2263-31/4. The study is registered under EudraCT 2015-000630-30 and NCT02579252. The EudraCT is the primary record.

Study design and participants

The study enrolled subjects with a diagnosis of probable AD according to the 2011 NIA-AA criteria (McKhann, 2011). Subjects were aged 50–85 years and had to have MMSE total score ≥ 20 and ≤ 26 at screening. Either evidence of medial temporal lobe atrophy (Scheltens score ≥ 2 on the more atrophied side) or a positive AD biomarker profile in the CSF (Aβ42 < 600 pg mL^{-1} *and* Aβ42/Aβ40 ratio < 0.089 *and* p-tau181 > 60 pg mL^{-1} *and* t-tau > 400 pg mL^{-1}), or both were required for enrolment. For the purpose of the present analysis, a simplified approach was used, with A+ status was defined as CSF Aβ42 < 600 pg mL^{-1} and T+ status as CSF p-tau181 $\geq$ 60 pg mL^{-1}.

The study was conducted at 41 sites in the European Union, in Austria, Czech Republic, Germany, Poland,

Romania, Slovakia, Slovenia, and Sweden. The study was a 24-month, randomised, placebo-controlled, double-blinded, parallel-arm trial. Subjects initially received 6 doses of AADvac1 or placebo at 4-week intervals, followed by 5 booster doses of AADvac1 or placebo at 14-week intervals.[2]

Interventions

Participants in the ADAMANT study were randomised 3:2 between AADvac1 or placebo. Each dose of AADvac1 consisted of 40 µg Axon Peptide 108 (tau 294–305/4R with added N-terminal cysteine, amino acid sequence CKDNIKHVPGGGS) coupled to keyhole limpet hemocyanin via a maleimide linker, adjuvanted with aluminium hydroxide (containing 0.5 mg Al^{3}+) in a phosphate buffer volume of 0.3 mL. The placebo consisted of adjuvant in phosphate buffer. Patients received up to 11 subcutaneous injections of AADvac1 or placebo, with the initial 6 doses being administered at 4-week intervals (weeks 0, 4, 8, 12, 16, and 20), and the 5 booster doses being administered at 14-week intervals (weeks 34, 48, 62, 76, and 90).

Randomisation and treatment masking

The AADvac1: placebo randomisation ratio was 3:2. The block size was 10. The placebo was identical in appearance to the investigational medicinal product.

An interactive web-based response system (IWRS) provided by Cenduit was employed. The randomisation sequence was generated by Cenduit. The IMP vials were identified using unique vial numbers. Prior to administration, the investigator contacted the IWRS, which provided the number of the specific IMP vial that was to be administered.

Participants and all personnel involved in study conduct were blinded to treatment assignment of participants.

Cognitive and functional assessment

The CDR-SB and ADCS-MCI-ADL ("ADL") were assessed at weeks 0, 12, 24, 38, 52, 66, 80, 94, and 104. The MMSE was assessed at screening, and at weeks 12, 52, and 104. Computerised versions of the CDR, ADCS-MCI-ADL 24-item scale, and MMSE were employed, utilising the MedAvante Virgil platform (MedAvante, NJ, USA). The tests were administered and scored by site raters.

Analysis methods of neurodegeneration endpoints

Immunogenicity was assessed at every post-baseline visit—i.e., at 4- to 10-week intervals, as described previously.[2] Briefly, area under the curve (AUC) of each participant's longitudinal immunogenicity curves were calculated and used as a representation for antibody production.

Concentrations of NfL in plasma were measured using single molecule array (Simoa) digital ELISA,

using an HD-1 Analyzer (v1.5) and the NF-Light Advantage assay (Quanterix). Each measurement was performed in duplicate according to manufacturer recommendations.

MRI was collected at 3T field strength with the whole brain as area of acquisition. One or two combined scout scans were done (T1-weighted axial scout, T1-weighted coronal scout, T1-weighted sagittal scout) to serve exact repositioning in follow-up examinations. Parameters for T1W 3D scans were as follows: MPRAGE or T1-TFE, 1 mm isotropic resolution with whole brain coverage. 3D T1 scans were normalised by nonlinear registration to a template. All scans that were affected by noise and motion artifacts were repeated or excluded from analysis. No volume censoring was performed. Regional volumes of bilateral temporal lobe, left and right hippocampus, lateral ventricles, and whole cortex were subsequently extracted from the processed brain scans, and analyzed. Whole brain volume loss was calculated with SIENA 2.6 (part of FMRIB Software Library (FSL), Oxford Centre for Functional MRI of the Brain). Anatomical locations were determined from automated labelling with FreeSurfer. To extract volume estimates of individual regions of interest, images were automatically processed with the longitudinal stream in FreeSurfer (v.6.0).

These markers of neurodegeneration—NF-L and MRI—were analysed at weeks 0, 52, and 104 to ensure comparability between changes in the biomarkers and to reflect the focus on viable lengths of future trials being 12 or 24 months.

Concentrations of t-tau and p-tau T181 and concentrations of amyloid-β1-40 and amyloid-β1-42 were measured in CSF using Innotest ELISA assays (Fujirebio, Japan). The amyloid-β 1–42/1–40 ratio was measured via the Mesoscale Discovery platform (MD, USA).

Machine learning model

A methodology developed by Tosun and colleagues was employed for imputing brain amyloid-positivity (A+) and tau-positivity (T+) status of study participants.[4–7] This approach used N = 6287 structural MRI scans of N = 1296 unique participants from the Alzheimer's Disease Neuroimaging Initiative (ADNI1-3) studies with known Aβ-positivity status based on either CSF or PET imaging, and tau-positivity status based on CSF p-tau, together with demographics (age, sex, years of education and APOE genotype) and baseline CDR-SB score to train a deep-learning (DL) model. Participants with missing information were excluded from the study. Aβ-positivity status based on either CSF or PET imaging and tau-positivity status based on CSF p-tau were selected as the ground truth reference standard to maximize the sample size. Structural MRI scans were minimally processed to remove non-brain tissue and rigid register to MNI image coordinate. The image files were de-identified during transfer from clinical imaging site to data centre, in accordance with HIPAA regulations and ensuring that no identifiable subject information crosses the network. A multi-task model for predicting A-positivity and T-positivity labels simultaneously was trained using a UNet architecture,[8] consisted of 18 3D convolution layers split into 9 convolution blocks and terminated with 3 fully connected layers. The convolution blocks contain two convolutional layers, each followed by a batch normalisation layer and ReLU activation. Each block had skip connection inspired by ResNet, which is a pointwise addition of the output of the first convolutional layer and the second convolution layer. After the first and fourth convolutional blocks a pool size of $2 \times 2 \times 2$ and a stride of 2 was used at the average pooling layer. The UNet feed forward connections were accomplished by concatenating $2 \times 2 \times 2$ upsampled layers. The convolution blocks were followed by a global average pooling layer and three fully connected layers. The first two fully connected layers had ReLU activation functions while the final fully connected layer had no applied activation function. The data set was divided into 50% training, 25% internal testing, and 25% internal validation sets based on unique subjects in the dataset. Model was trained using stochastic gradient descent with 0.9 momentum for a maximum of 100 epochs and early stopping based on testing set softmax cross entropy loss was used to select models for independent validation. The fully trained DL model was first independently tested on a validation cohort of 340 unique ADNI1-3 participants with mild-to-moderate AD, aged between 54 and 85 years, followed by a final independent and blinded validation in a subset of 46 ADAMANT participants who had CSF biomarker assessment at baseline. The method yields individual level probabilistic scores for amyloid-positivity and tau-positivity, with values ≥0.5 interpreted as amyloid- and tau-positive (i.e., "A+T+"). This model was then applied to participants in the ADAMANT trial, blinded to both treatment allocation and any follow-up information.

Statistics

The significance level was set at p < 0.05; results with p < 0.1 were considered trends.

Sample size

Given a 3:2 AADvac1 to placebo allocation with at least 135 subjects (81:54) expected to complete the study, the ADAMANT study was powered to show a standardised difference of 0.5 as statistically significant with a power of 0.80 and at the significance level of 0.05 using a two-sided two-sample Student t-test; correcting for a 25% dropout, 180 subjects (108:72) were targeted for randomisation.

No power calculation was performed for the present analysis—all patients fulfilling the CSF criteria or

identified by the machine learning model were used for analysis. A total of 119 patients were identified for this analysis (AADvac1 n = 70; Placebo n = 49).

MMRM
Analysis of trial endpoints (CDR-SB, ADCS-ADL, NF-L, MRI) was performed using a mixed model for repeated measures (MMRM) with study visit treated as a categorical variable. The MMRM was fit using restricted maximum likelihood estimation and an unstructured correlation matrix, and was adjusted for treatment status, baseline outcome, age, sex, geographical region, baseline MMSE, *APOE* status, and disease severity as measured by baseline plasma NF-L. An interaction effect was also included between the categorical time variable and all covariates to account for the potential that covariates may not be perfectly randomized after selection by the machine learning model. Estimated marginal means were subsequently calculated to determine the effect of treatment on outcome at the 104-week study visit, and with exploratory analysis of intermediate visits. The Kenward–Roger approximation was used to estimate denominator degrees of freedom. No imputation for missing data was performed and the missing-at-random principle was assumed.

Finally, total antibody production adjusted for sex, age, and baseline of the given endpoint was investigated as a predictor of endpoint change from baseline in the treatment group using robust linear regression. All endpoints were analysed in separate models.

Model development and prediction of A+T+ status was performed using the Python programming language (v3.4). All other statistical analyses were performed using the R programming language (v4.0.5) and GraphPad Prism (v8.4.3) with a significance level of 0.05 and without correction for multiple comparisons due to the exploratory nature of the analysis.

Role of the funder/sponsor
AXON Neuroscience was involved in the design of the study; in the collection, analysis and interpretation of data; and in the writing of this report. The corresponding author had full access to all data and had final responsibility for submission of the report for publication.

Results
Overall participant characteristics
The demographics of the full sample are presented in,[2] and replicated in the Supplementary Materials. Briefly, 196 participants were randomised in a 3:2 treatment allocation, with 193 participants composing the full analysis set under the modified intention-to-treat principle due to having at least one post-baseline endpoint assessment.

Levels of CSF Aβ42, p-tau T181, and t-tau were available at baseline in 46 of 193 (23.8%) participants. In

this CSF subgroup, 44 of 46 (97.8%) participants had abnormal levels of CSF Aβ42 ("CSF A+"; cutoff <600 pg/mL), while 32 of 46 (69.6%) participants had both abnormal levels of CSF p-tau ("CSF T+"; cutoff ≥60 pg/mL) and CSF Aβ42. Furthermore, another 14 participants provided CSF samples at post-baseline visits only, with 10 of 14 participants having abnormal levels of both CSF Aβ42 and CSF p-tau. Together, 42 of 60 (70%) participants with available CSF measurements had abnormal levels of both CSF Aβ42 and CSF p-tau ("CSF A+T+") and were carried forward for further analysis.

Validation of A+T+ prediction model
The fully trained ML risk model was validated in a subset of 46 participants who had CSF Aβ42 and CSF p-tau T181 biomarker available at the baseline visit. The CSF sub-group data was not used to directly adjust or optimise the ML model parameters and authors working on the ML model were blinded to CSF sub-group identification and CSF biomarker results. In predicting abnormal CSF Aβ42 status in the CSF sub-group, the ML risk model achieved a positive predictive value (PPV) of 97.7% (CI [91.4%, 99.4%]; i.e., 43 true positive (TP)/44 TP + false positive (FP)) and a negative predictive value (NPV) of 50.0% (CI [8.4%, 91.5%]; i.e., 1 true negative (TN)/2 TN + false negative (FN)). In predicting CSF p-tau status, the model had a PPV of 96.2% (CI [78.9%, 99.4%]; i.e., 25 TP/26 TP + FP) and an NPV of 65.0% (CI [48.7%, 78.4%]; i.e., 13 TN/20 TN + FN). The combination similarly had a PPV of 96.2% (CI [78.9%, 99.4%]; i.e., 25 TP/26 TP + FP).

For abnormal CSF p-tau status, the model had a sensitivity of 78.1% (CI [43.8%, 100.0%]), and a specificity of 92.9% (CI [55.5%, 100.0%]); for abnormal CSF Aβ42 status, sensitivity and specificity estimates on larger samples were reported previously[4]; in the present study, the model had a sensitivity of 95.5% (CI [57.6%, 100.0%]), and a specificity of 50.0% (CI [22.5%, 77.5%]; one out of two CSF Aβ42-negative patients was incorrectly classified as positive by the algorithm) (see Table 1).

Use of A+T+ prediction model
To impute the A+T+ status in the remaining 133 of 193 full analysis set (FAS) participants who did not have CSF Ab42 and CSF p-tau181 biomarker levels available, a validated ML model as described above was employed.

The fitted ML model was applied to all ADAMANT participants who did not have available CSF biomarker data for the purpose of inferring A+T+ status. As a result, 77/133 participants without available CSF biomarker data were inferred to be A+T+ using the ML model and carried forward for further analysis.

A+T+ participant characteristics
A total of 119 participants were identified as A+T+ through abnormal CSF Ab42 and p-tau levels or through inference by the ML risk model (Fig. 1); 116/119 also

	CSF amyloid-β1-42 (A+)	CSF pTau pT181 (T+)	Combined (A+T+)
Sensitivity	95.5%	78.1%	78.1%
Specificity	50.0%[a]	92.9%	92.9%
PPV	97.7%	96.2%	96.2%
NPV	50.0%	65.0%	65.0%

[a]One out of two A– patients was labelled as A+ by the algorithm.

Table 1: Sensitivity, specificity, and positive and negative predictive values of the machine learning algorithm in the ADAMANT population.

qualified as N+, having a Scheltens hippocampal atrophy score of 2 or higher. Demographics of this subgroup analyses were well balanced. The average age was 70.8 years (8.41) in the AADvac1 treatment group compared to 71.9 (7.19) in the placebo group, the average years of education were 12.8 (3.29) in the treatment group versus 12.1 (2.99) in the placebo group, with 58.6% female participants in the treatment group compared to 59.2% in the placebo group, and with the average baseline MMSE score was 22.8 (1.93) in the AADvac1 treatment group versus 23.0 (1.98) in the placebo group. There were no statistically significant differences in baseline characteristics for the covariates between treatment and placebo groups in the A+T+ group (Table 2).

Analysis of cognitive and functional endpoints
Based on an MMRM analysis in A+T+ participants, trends towards statistically significant treatment effects were noted at 104 weeks for change from baseline in CDR-SB (estimated marginal means [emm] = −0.99 points, 95% CI [−2.13, 0.13], p = 0.0825, df = 432) in ADL (emm = 3.82 points, CI [−0.29, 7.92], p = 0.0679, df = 427) (Fig. 2A and B). When considering intermediate study visits, there was also a trend towards reduction of clinical decline in the treatment group compared to the placebo group for CDR-SB at week 52 (emm = −0.66 points, CI [−1.38, 0.07], p = 0.0744) and at week 80 (emm = −0.80 points, CI [−1.76, 0.17], p = 0.1048). For ADL, a statistically significant reduction of decline in the treatment group compared to placebo group was noted at week 52 (emm = 3.96 points, CI [0.71, 7.22], p = 0.0176) (Fig. 2A and B).

A sensitivity analysis was performed with the same MMRM approach in the subgroup of participants who had CDR-SB and ADL evaluated at the final, 104-week study visit (completers, n = 99 (df = 393) for ADL and n = 101 (df = 401) for CDR-SB). In this group, there was a statistically significant reduction of decline for the treatment group in CDR-SB evaluated at week 52 (p = 0.0447) and trends at week 80 (p = 0.0574) and 104 (p = 0.0532) (Fig. 2C). Similarly, there was a statistically significant reduction of decline for the treatment group in ADL evaluated at week 104 (p = 0.0459) and week 52 (p = 0.0097), with a trend at week 80 (p = 0.0936)

(Fig. 2D). All results are also presented in their entirety in Supplementary Table S4.

Analysis of neurodegeneration biomarkers
Endpoints related to neurodegeneration—plasma NF-L and MRI measures—were analysed using the same MMRM analysis as described above, but with whole brain volume added as an additional covariate for MRI measures. For the neurodegeneration endpoints the MMRM analysis showed a statistically significant difference between treatment and placebo groups at 104 weeks in change from baseline in plasma NF-L (emm = −0.15 log pg/mL, CI [−0.27, −0.03], p = 0.0139, df = 216). There was a statistically non-significant reduction in temporal lobe volume-loss (emm = 2.1 absolute %, CI [−0.93, 5.12], p = 0.1720, df = 209) and whole brain cortical volume loss for the treatment group compared to the placebo group at week 104 (emm = 1.53 absolute %, CI [−0.96, 4.02], p = 0.2249, df = 209) (Fig. 3A–C).

Analysis of completers for these endpoints showed a statistically significant reduction in plasma NF-L levels at week 104 for the treatment group (p = 0.0172, df = 206) and a statistically non-significant reduction for temporal lobe volume (p = 0.2485, df = 196) and cortical volume loss (p = 0.3192, df = 196) (Fig. 3D–F). There were no differences between treatment and placebo groups at weeks 52 or 104 for any of the other MRI endpoints (left and right hippocampus, ventricles, Supplementary Figure S1). All results are also presented in their entirety in Supplementary Table S4.

Relationship between trial endpoints and antibody production
In evaluating the treatment effects of AADvac1 in the A+T+ population, the correlations between cumulative AADvac1-induced anti-tau antibody production over the study period of 104-week, and change from baseline at 104 weeks for all outcomes (CDR-SB, ADL, plasma NF-L, and MRI volumetry) were calculated. Included in this further sub-analysis were 62 AADvac1-treated participants who had endpoint values at the 104-week visit. Robust linear regression modelling adjusting for age, sex, and baseline value of the endpoint demonstrated a statistically significant association of total AADvac1-induced anti-tau antibody production with change
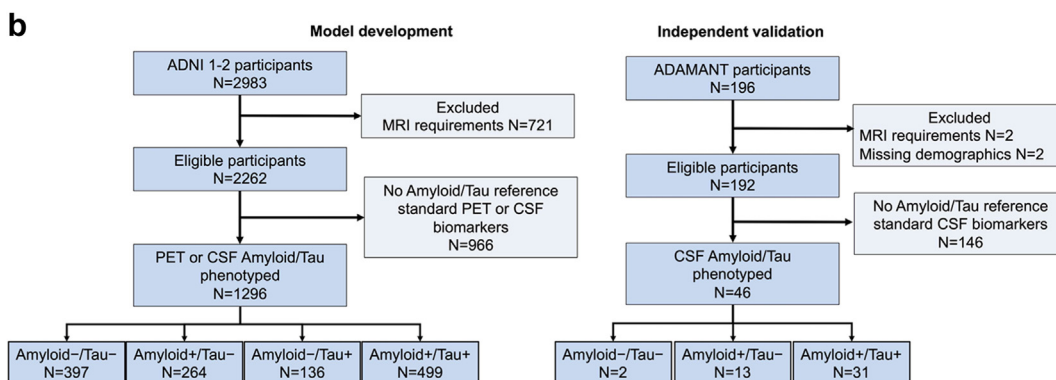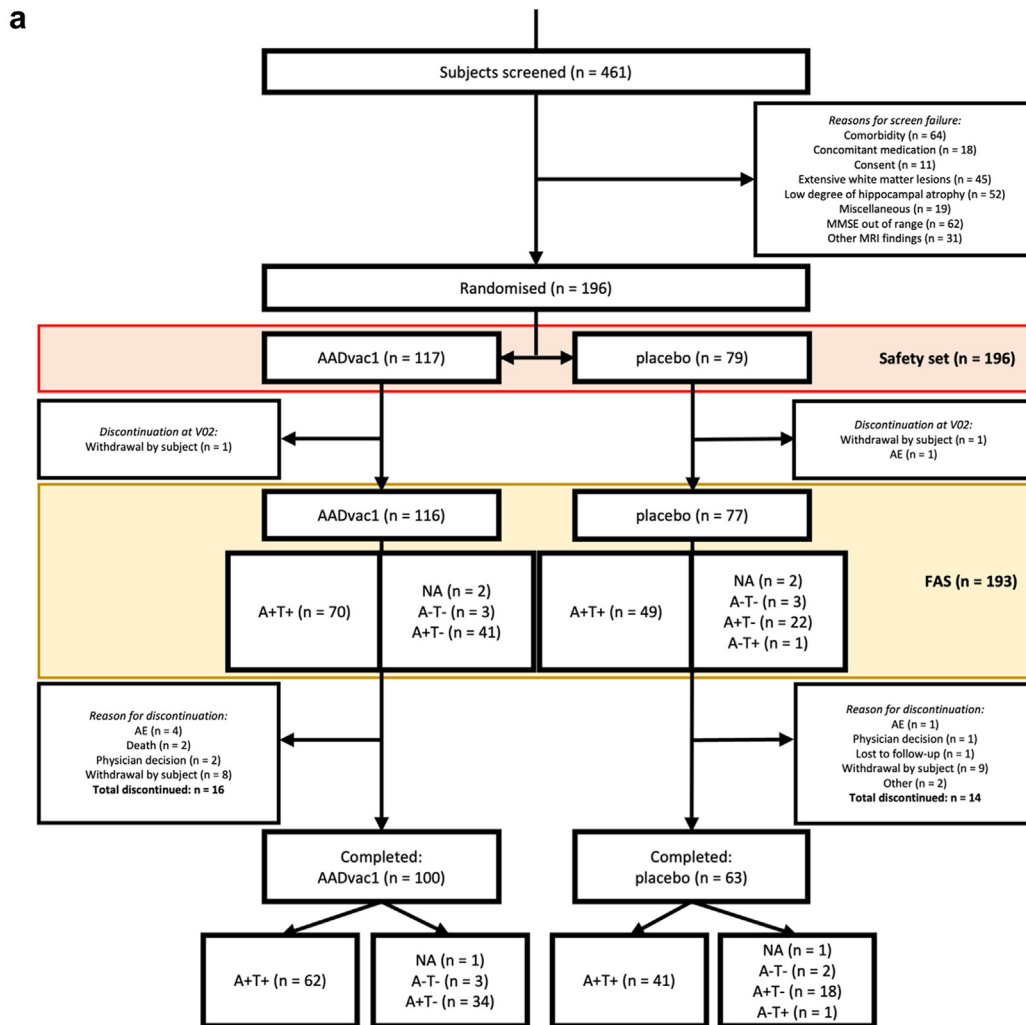
a

b

Fig. 1: Diagrams of study design (CONSORT and STARD flowchart). (a) CONSORT flowchart. FAS = full analysis set. NA = patient could not be evaluated by the machine learning algorithm and did not provide CSF. The FAS are all patients who have any post-baseline value for efficacy; completers are FAS patients who have attended the end-of-study visit at week 104. Patients could present with multiple reasons for screening failure. (b) STARD flowchart. Flow diagram of participants and Amyloid/Tau phenotype of participants within the ADNI model development cohort and within the ADAMANT independent validation cohort.

	AADvac1 (n = 70)	Placebo (n = 49)
Age (years) (median, quartiles, range)	73.0 (IQR 64.5–77.0; range 53–84)	73.0 (IQR 66.5–77.0; range 51–83)
Time since AD diagnosis (months) (median, quartiles, range)	9.0 (IQR 4.0–23.0; range 3–134)	15.0 (IQR 5.0–26.00; range 3–55)
Sex (% male/female)[a]	41.4/58.6	40.9/59.1
Ethnic origin (%)	Caucasian: 100.0	Caucasian: 100.0
Education (years) (median, quartiles, range)	12.0 (IQR 10.0, 16.0; range 7–18)	12.0 (IQR 10.0–13.0; range 6–19)
Concomitant AChEI treatment (n, %)	70 (100.0)	49 (100.0)
Concomitant memantine treatment (n, %)	17 (24.3)	11 (22.5)
MMSE (mean, SD)	22.8 (1.93)	23.04 (1.98)
CDR-SB (mean, SD)	4.3 (1.92)	4.8 (2.47)
ApoE4 (n, %)	Non-carrier: 27 (38.6%) Heterozygote: 33 (47.1%) Homozygote: 10 (14.3%)	Non-carrier: 12 (24.5%) Heterozygote: 30 (60.2%) Homozygote: 7 (14.3%)
Hippocampal atrophy score (n, %)	Scheltens 0: 0 (0%) Scheltens 1: 3 (4.3%) Scheltens 2: 40 (57.1%) Scheltens 3: 22 (31.4%) Scheltens 4: 5 (7.1%)	Scheltens 0: 0 (0%) Scheltens 1: 0 (0%) Scheltens 2: 30 (61.2%) Scheltens 3: 14 (30.0%) Scheltens 4: 5 (10.2%)
White matter lesion score (n, %)	Fazekas 0: 12 (17.1%) Fazekas 1: 43 (61.4%) Fazekas 2: 15 (21.4%) Fazekas 3: 0 (0%)	Fazekas 0: 9 (18.4%) Fazekas 1: 28 (57.1%) Fazekas 2: 12 (24.5%) Fazekas 3: 0 (0%)
Neurofilament light chain protein in plasma (pg/mL, mean and 95% CI)	22.06 (20.07, 24.04)	20.15 (18.19, 22.10)

[a]Biological sex.

Table 2: Demographics of the A+T+ subset.

from baseline at 104 weeks in CDR-SB (rho = −0.10, CI [−0.21, 0.01], p = 0.0376. Fig. 4A), ADL (rho = 0.15, CI [0.03, 0.27], p = 0.0201, Fig. 4B) and volume loss in the left hippocampus (rho = 0.35, CI [0.28, 0.43], p < 0.0001, Fig. 4E) and right hippocampus (rho = 0.27, CI [0.17, 0.37], p = 0.0057, Fig. 4F), temporal lobe volume loss (rho = 0.30, CI [0.22, 0.38], p < 0.0001, Fig. 4G), and whole cortical volume loss (rho = 0.18, CI [0.10, 0.26], p = 0.0044, Fig. 4H), but no association with plasma NF-L (rho = 0.01, CI [−0.15, 0.16], p = 0.9266, Fig. 4C) and ventricles (rho = −0.16, CI [−0.35, 0.04], p = 0.2477, Fig. 4D). The consistency of the findings is also supported by mutual correlations among 104-week change from baseline for both cognitive endpoints and temporal lobe volume (p = 0.0006 and < 0.0001, respectively, see Supplementary Materials results).

Discussion

In this exploratory post hoc analysis of the ADAMANT trial of AADvac1, an active peptide vaccine targeting pathological tau in AD, a complex machine learning algorithm including volumetric MRI combined with other factors including APOE, demographics and baseline cognitive performance is used to identify a subgroup of participants who were likely to be classified as A+ T+ by CSF criteria. This predictive modelling was able to identify a subgroup of trial participants among those who did not contribute CSF but whom this algorithm classified as being putatively A+ and T+. This AD

biomarker identification expands the available CSF-positive sample of participants to explore treatment effects in those enriched for having a higher likelihood of AD while also excluding those with lower likelihood. In this study we find that maximising positive predictive value is the preferred strategy for such algorithms, as including false positives can greatly undermine interpretation of results and statistical power. We also show that leveraging openly available cohorts such as ADNI, in combination with validating ground-truth CSF or PET data, is vital to ensuring model accuracy. In this way, observational cohorts can inform and improve analysis of clinical trials in AD.

By using a machine learning model, we identified A+T+ participants in our study and performed an MMRM analysis with multiple endpoints—cognitive (CDR-SB), functional (ADL), and biomarkers of neurodegeneration (plasma NF-L and brain atrophy measured using MRI). Here, we demonstrate that treatment with AADvac1 appears to slow disease progression across four key endpoints. The treatment effect appears most apparent in 68% slow-down of accumulation of plasma NF-L, which is a marker of general neurodegeneration and shows potential as both a disease progression marker in AD[9,10] and as a marker of treatment response. While lacking specificity for any specific neurodegenerative disease it has shown treatment responsiveness in Huntington's disease, spinal muscular atrophy, and amyotrophic lateral sclerosis.[11,12] The CDR-SB and ADCS-MCI-ADL are widely employed as clinical
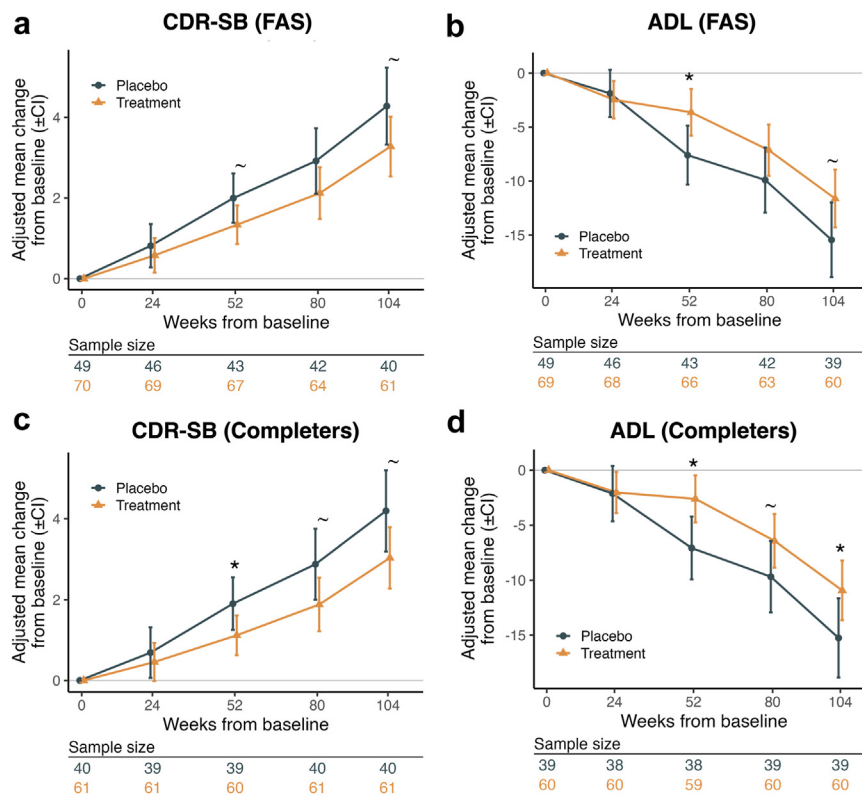
Fig. 2: **MMRM analysis of cognitive and functional endpoints.** This figure shows the results of a mixed model for repeated measures (MMRM) analysis for CDR-SB and ADCS-ADL endpoints, with p-values derived from estimated marginal means. All models were adjusted for the baseline and time-interaction effects of age, sex, geographical region, baseline MMSE, baseline plasma NF-L, and *APOE* status. Higher CDR-SB values and lower ADL values indicate worsening. (a and b) Full analysis set (n = 119). (c and d) Analysis of completers (participants who had CDR-SB and ADL evaluated at the final, 104-week study visit). Error bars indicate standard error and the dotted line indicates baseline. The number of participants for at each visit is presented under each figure. These results are also presented in Supplementary Table S4. ~p < 0.1; *p < 0.05.

outcome measures in AD trials; and would be expected to be less sensitive to treatment effects than biomarkers.[13] AADvac1 slowed disease progression by 23% (CDR-SB) and 25% (ADCS-MCI- ADL) at 104 weeks in this A+T+ subgroup. Such effect size resembles that of anti-amyloid antibodies, donanemab (23% on CDR-SB, 23% on ADCS-iADL at 76 weeks) and lecanemab (22% on CDR-SB, 40% on ADCS-MCI- ADL at 78 weeks); effects of this size are generally considered clinically meaningful in AD. AADvac1 did not show a statistically significant slowing down of brain atrophy as assessed via MRI volumetry–most importantly though, the vaccine did not contribute to a decrease in brain volume, which has been observed in several anti-amyloid therapies.[14,15]

In understanding treatment effects of active immunotherapy, it is also important to evaluate the relationship between treatment response and antibody levels. These further exploratory analyses suggest that the cumulative AADvac1-induced anti-tau antibody production over the study period within the A+T+ participants is correlated with a reduction in the rate of decline on

cognitive and functional endpoints, and with reduced brain atrophy. This relationship suggests that more antibody production in participants results in a better treatment effect, analogously to dose-dependent effects with other therapeutics. The correlations were weak to moderate, which is in line with the notion that numerous factors affect the relationship between the dose of a therapeutic and its impact on the disease, and AD is a very heterogeneous disorder.[16] The factors affecting the relationship antibody response and effect would need to be explored in further studies to identify populations who benefit most and least.

The present study also demonstrates that it is possible to impute A+T+ status in AD participants by using a machine learning model. While the CSF p-tau T181 biomarker used to validate the machine learning model is a measure of the presence of AD neuropathologic change, and not necessarily a quantitative measure of tau pathology, it is specific to AD, and suitable to rule out cases where progressive amnestic syndrome and hippocampal atrophy are mostly caused by other neuropathologies, such as Limbic-predominant age-
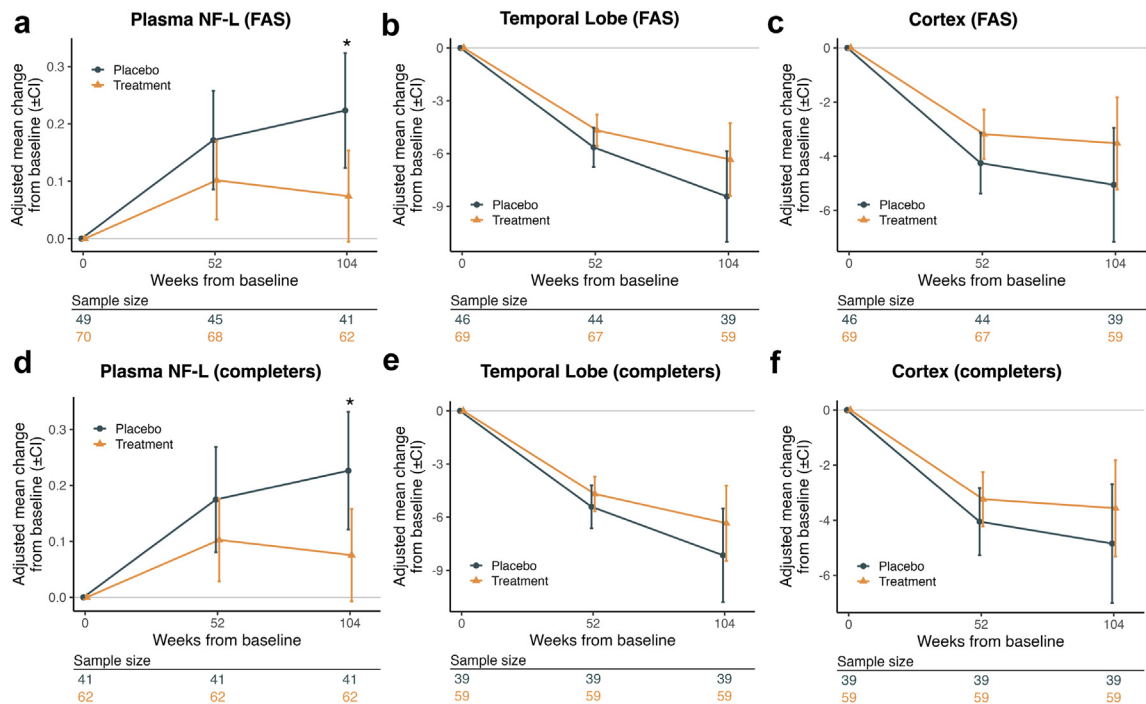
Fig. 3: MMRM analysis of neurodegeneration endpoints. This figure shows the results of a mixed model for repeated measures (MMRM) analysis for plasma NF-L and MRI (volume of, temporal lobe, and whole cortex) endpoints for the Full Analysis Subset in sub-figures (a–c) (n = 119) and the set of participants who had endpoint evaluations at the final, 104-week study visit in sub-figures (d–f) (completers). p-values are derived from estimated marginal means. All models were adjusted for the baseline and time-interaction effects of age, sex, geographical region, baseline MMSE, and *APOE* status. Error bars indicate standard error and the dotted line indicates baseline. The number of participants for at each visit is presented under each figure. These results are also presented in Supplementary Table S4. *p < 0.05.

related TDP-43 encephalopathy (LATE)[17]; thus, it is fit for the purpose of the present analysis. Recently, blood-based biomarkers showed great potential for AD diagnosis.[18] They are already recommended for pre-screening for individuals likely to have AD for their inclusion into clinical trials[18] and potentially even for tracking treatment response during the trial itself. The ML model used in our study might be further optimised by including plasma biomarkers. The combination could provide a highly accurate model with superior performance metrics.

Limitations
Given that the present study was performed post-hoc, and not pre-specified in the study protocol, these results must be seen as being exploratory and hypothesis generating. The ground-truth biomarker data (i.e., CSF or PET) for the imputed A+T+ cohort is not available. Therefore, it is likely that some participants in the inferred A+T+ group may not have been included if these data were available. The machine learning algorithm needs further validation with other cohorts. Moreover, while CSF data was available in a small subset of the A+T+ participants in our study—and was utilised when possible—the CSF subgroup was too

small to perform any meaningful analysis in terms of treatment effect.

There are possible sources of confounding that cannot be accounted for in this analysis—for example, it is conceivable that the correlation between antibody response and slowing of brain atrophy or cognitive decline could be explained by differences in immuno-logical health of the patients impacting both the anti-body response and e.g., brain atrophy rate. As with all post-hoc studies, the present analysis cannot eliminate some potential sources of bias; the generalizability of a Phase 2 trial of this size is also somewhat limited e.g., due to the generally stricter inclusion criteria used in Phase 2 studies compared to Phase 3 trials.[19] The proof of the utility of these post hoc analyses will require further testing with prospective A+T+ inclusion criteria within a randomised controlled clinical trial.

Conclusions
In the present study, we showed that a machine learning model combining MRI with cognition and demography potentially could be effectively utilised to impute the presence of Aβ and tau pathology (A+T+) of trial participants. Moreover, we also showed that an anti-tau therapy had potentially positive treatment effects in
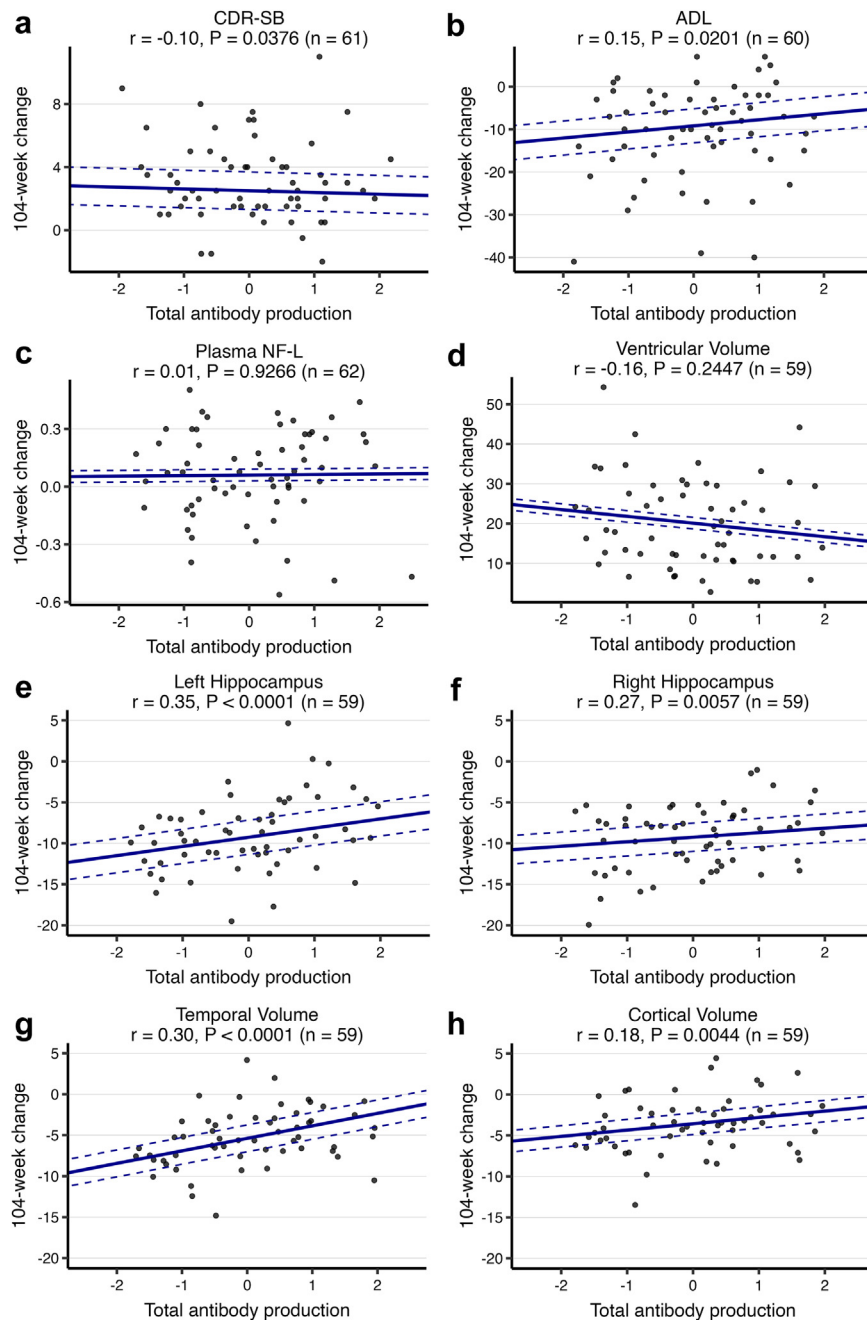
Fig. 4: AADvac1-induced anti-tau antibody production versus change in trial endpoints. This figure shows the results of linear regression modelling with AADvac1-induced anti-tau production as independent variable and change from baseline at 104 weeks in trial endpoints (a: CDR-SB, b: ADCS-ADL, c: plasma NF-L, and MRI [volumes of d: lateral ventricles, e and f: hippocampi, g: temporal lobe, and h: whole cortex]) as dependent variables. AADvac1-induced anti-tau antibody production is presented on a natural logarithmic scale and was adjusted for age and sex before analysis. Only participants from the treatment group who completed the 104-week visit were included in the analysis (n = 62). The number of participants for each analysis is presented in the figure sub-headers.

this A+T+ subgroup across several cognitive, functional, and biomarker endpoints. We provide some evidence that the response to treatment may be directly related to total AADvac1-induced anti-tau antibody production. Taken together, our results suggest that larger scale anti-tau trials with AADvac1 in AD patients with a priori confirmation of both amyloid and tau pathology (i.e., A+T+) are both needed and warranted.

The above are the results of a post-hoc analysis, with ground-truth biomarkers being unavailable in a portion of patients. Post-hoc analyses cannot eliminate some potential sources of bias. Some of the conclusions of this study are based on small-to-moderate sample sizes. The findings require confirmation in another study.

Contributors
Nicholas Cullen: statistical analysis, manuscript preparation.

Petr Novak: clinical trial design, interpretation of results, manuscript preparation.

Duygu Tosun: development of the machine learning model, application of said model on present patient sample.

Branislav Kovacech: led investigational medicinal product (IMP) design, and contributed to data analysis and interpretation and manuscript preparation.

Jozef Hanes: biomarker analysis.

Reinhold Schmidt: coordinating investigator, interpretation of results.

Stefan Ropele: MRI setup and coordination, volumetry.

Howard Feldman: analysis plan for the study, interpretation of results.

Eva Kontsekova: immunogenicity analyses.

Bengt Winblad: study design, interpretation of results.

Norbert Zilka: clinical trial design, interpretation of results.

Michal Fresser: clinical trial oversight.

All authors read and approved the final version of the manuscript. Nicholas Cullen and Petr Novak have verified the data. Norbert Zilka approved the manuscript for submission.

Data sharing statement
All data and code from the present study is available to qualified investigators upon relevant request and upon signature of a data access agreement. Individual participant data, data dictionaries, statistical code, study protocol and the statistical analysis plan will be made available following publication; investigator support will be provided, if necessary, based on the specified analysis. Please address data requests to office@axon-neuroscience.eu.

Declaration of interests
Nick Cullen received personal fees from AXON Neuroscience SE.

All authors affiliated with AXON NEUROSCIENCE SE or one of its subsidiaries received salary from their respective companies.

Jozef Hanes, Eva Kontsekova, and Branislav Kovacech report patents with AXON Neuroscience R&D Services SE.

Petr Novak received payments from F. Hoffmann-La Roche AG.

The investigators' institutions received reimbursement on a per-patient per-visit basis.

Duygu Tosun's institution received payments from AXON Neuroscience for image processing, and payments to the institution from Siemens Medical Solutions USA, Inc., Takeda Pharmaceutical Company Ltd., DOD WW81XWH-19-1-0669, NIH/NIA U19AG024904, NIH/NIA U01AG068057, NIH/NIA U24AG074855, NIH/NIA R01AG058676.

Reinhold Schmidt has received personal fees and honoraria for image analyses from AXON NEUROSCIENCE.

Stefan Ropele reports no conflict of interest.

Bengt Winblad reports personal fees for taking part in Scientific Advisory Board meetings and Data Safety Management Board meetings from AXON NEUROSCIENCE, and from Alzinova DSMB and Artery TX SAB.

Dr. Feldman reports a service agreement between Axon Neuroscience and UCSD for consulting and travel with all payments to UCSD and no personal funds received. Other activities to report include: grant funding from Annovis (QR Pharma), Vivoryon (Probiodrug), AC Immune, and LuMind; service agreements for consulting activities with LuMind, Genentech (DSMB), Roche/Banner (DMC), Tau Consortium (SAB), Samus Therapeutics, Biosplice Therapeutics, Novo Nordisk Inc., Janssen Research & Development LLC, and Arrowhead Pharmaceuticals with no personal funds received and all payments to UCSD. He also reports a philanthropic donation to UCSD from the Epstein Family Alzheimer's Disease Collaboration for therapeutic research in AD.

References
1 Kontsekova E, Zilka N, Kovacech B, Novak P, Novak M. First-in-man tau vaccine targeting structural determinants essential for pathological tau-tau interaction reduces tau oligomerisation and neurofibrillary degeneration in an Alzheimer's disease model. *Alzheimers Res Ther*. 2014;6(4):44.

2 Novak P, Kovacech B, Katina S, et al. ADAMANT: a placebo-controlled randomized phase 2 study of AADvac1, an active immunotherapy against pathological tau in Alzheimer's disease. *Nat Aging*. 2021;1(6):521–534.

3 McKhann GM, Knopman DS, Chertkow H, et al. The diagnosis of dementia due to Alzheimer's disease: recommendations from the National Institute on Aging-Alzheimer's Association workgroups on diagnostic guidelines for Alzheimer's disease. *Alzheimers Dement*. 2011;7(3):263–269.

4 Tosun D, Chen YF, Yu P, et al. Amyloid status imputed from a multimodal classifier including structural MRI distinguishes progressors from nonprogressors in a mild Alzheimer's disease clinical trial cohort. *Alzheimers Dement*. 2016;12(9):977–986.

5 Tosun D, Joshi S, Weiner MW. Alzheimer's disease neuroimaging I. Neuroimaging predictors of brain amyloidosis in mild cognitive impairment. *Ann Neurol*. 2013;74(2):188–198.

6 Tosun D, Joshi S, Weiner MW, The Alzheimer's Disease Neuroimaging Initiative. Multimodal MRI-based imputation of the Abeta+ in early mild cognitive impairment. *Ann Clin Transl Neurol*. 2014;1(3):160–170.

7 Lang A, Weiner MW, Tosun D. O4-04-01: what can structural MRI tell about A/T/N staging? *Alzheimers Dement*. 2019;15(7S_Part_24): P1237–P1238.

8 U-net: convolutional networks for biomedical image segmentation. In: Ronneberger O, Fischer P, Brox T, eds. *International conference on medical image computing and computer-assisted intervention*. Springer; 2015.

9 Ashton NJ, Leuzy A, Lim YM, et al. Increased plasma neurofilament light chain concentration correlates with severity of post-mortem neurofibrillary tangle pathology and neurodegeneration. *Acta Neuropathol Commun*. 2019;7(1):5.

10 Moscoso A, Grothe MJ, Ashton NJ, et al. Longitudinal associations of blood phosphorylated Tau181 and neurofilament light chain with neurodegeneration in Alzheimer disease. *JAMA Neurol*. 2021;78(4): 396–406.

11 Yuan A, Nixon RA. Neurofilament proteins as biomarkers to monitor neurological diseases and the efficacy of therapies. *Front Neurosci*. 2021;15:689938.

12 Miller T, Cudkowicz M, Shaw PJ, et al. Phase 1-2 trial of antisense oligonucleotide tofersen for SOD1 ALS. *N Engl J Med*. 2020;383(2): 109–119.

13 Cummings JL. Integrating ADNI results into Alzheimer's disease drug development programs. *Neurobiol Aging*. 2010;31(8): 1481–1492.

14 Ayton S. Brain volume loss due to donanemab. *Eur J Neurol*. 2021;28(9):e67–e68.

15 Decourt B, Noorda K, Noorda K, Shi J, Sabbagh MN. Review of advanced drug trials focusing on the reduction of brain beta-amyloid to prevent and treat dementia. *J Exp Pharmacol*. 2022;14:331–352.

16 Tosun D, Demir Z, Veitch DP, et al. Contribution of Alzheimer's biomarkers and risk factors to cognitive impairment and decline across the Alzheimer's disease continuum. *Alzheimers Dement*. 2022;18(7):1370–1382.

17 Nelson PT, Dickson DW, Trojanowski JQ, et al. Limbic-predominant age-related TDP-43 encephalopathy (LATE): consensus working group report. *Brain*. 2019;142(6):1503–1527.

18 Hansson O, Edelmayer RM, Boxer AL, et al. The Alzheimer's Association appropriate use recommendations for blood biomarkers in Alzheimer's disease. *Alzheimers Dement*. 2022;18: 2669–2686.

19 Baldwin JR, Pingault JB, Schoeler T, Sallis HM, Munafo MR. Protecting against researcher bias in secondary data analysis: challenges and potential solutions. *Eur J Epidemiol*. 2022;37(1): 1–10.